Engineering and Technology Journal
Journal homepage: https://etj.uotechnology.edu.iq

Experimental study of the double pipe heat exchanger for heat transfer and pressure drop characteristics of the grooved tube

Natiq A. Fadhil[a,b*], **Aamer M. Al-dabagh**[b], **Falah F. Hatem**[b]

[a] Electromechanical Engineering Dept., Faculty of Engineering, University of Samara, Iraq.
[b] Mechanical Engineering Dept., University of Technology-Iraq, Alsina'a street, 10066 Baghdad, Iraq.
*Corresponding author Email: eng.natiq6813@gmail.com

HIGHLIGHTS

- A double-pipe heat exchanger was fabricated, employing heated water as the working fluid.
- The Nusselt Number exhibited a notable increase, ranging from 25% to 59%.
- Pressure drops demonstrated a significant rise, with an increase in (e/dh) ranging from 66% to 130%.

ARTICLE INFO

Handling editor: Ayad M. M. Jubori

Keywords:
Corrugated tube
Heat transfer enhancement
Rod baffle
Friction factor
Nusselt number
Heat exchanger
Pressure drop

ABSTRACT

Experiments are conducted to investigate the heat transfer and pressure drop characteristics of corrugated tubes and rod baffles in a shell-and-tube heat exchanger. One of the effective techniques to improve heat transfer is to use corrugated tubes. This article investigates rod baffles with varied corrugation depths and corrugated tubes for (1 start). In the heat exchanger's shell side, where a constant wall temperature was attained on the tube side, water was employed as the working fluid after being heated at the wall. Corrugation ratios (e/dh) of 0.1 and 0.13, pitch (p) of 10, 20, and 30mm, and two types (x/d) of 1.25 and 1.375 were used. The study was conducted throughout the Reynolds number turbulent range (4,000 to 24,000). The results manifested that the average Nusselt number of the corrugated tubes (pitch-10mm) for (x/d=1.25) increased by 25 and 55 percent for the corrugation depths of 0.1 and 0.13, respectively. The average Nusselt number for (x/d=1.375) is increased by 38% and 59% for the corrugation depths of 0.1 and 0.13, respectively. Nevertheless, the average friction factor of the corrugated tube with (e/dh) = 0.1 and 0.13 is higher than that of the smooth tube by 66% and 130%, respectively, and it decreases as the corrugation pitch and (x/d) are increased. When a corrugated tube and a rod baffle with a corrugated depth (e=2.1 mm) and pitch (p=10 mm) were used, the thermal enhancement factor was 1.9 for (x/d=1.25) and 1.97 for (x/d=1.375) at the same pumping power.

1. Introduction

The study investigates using corrugated tubes and rod baffles to enhance shell-side heat transfer in tubular heat exchangers, a solution applicable to multiple industries. Nowadays, there is a global issue regarding growing energy scarcity. In this regard, enhancing heat transmission is one way to increase energy effectiveness and conserve energy. There are several methods to improve heat transfer, and one effective method is to use tubes with intensified heat exchangers (HEs). In this particular field, many academics have made significant contributions.

In particular, the low heat transfer rate and the high-pressure drop in the shell side of the heat exchanger prompted researchers and heat exchange manufacturers to find an alternative to achieve the required change, which was in the form of the tubes and the baffle used inside the heat exchanger. This study emphasizes the significance of heat transfer performance in practical applications, the repercussions of inaccurate predictions, and the need for experimental data.

In this context, swirling turbulent gas-droplet flow in an abrupt expansion of a pipe was studied using a mathematical model created by Pakhomov and Terekhov [1], who discovered that the swirl increased heat transfer. Accordingly, the fins were positioned for Petracci et al. [2] finned cylinder to enhance the average heat transmission. In addition, the mean heat transfer upon a finned cylinder that was cooled via a rectangular jet was examined . In their study of the heat transfer behavior in circular and internally longitudinal finned tubes under laminar flow circumstances. Ravi et al., [3] found that the Stefan number, the fin thermal conductivity value, and the fin height substantially impacted the Nusselt number. In order to understand the regulating processes in the flow of a fin tube and to examine the turbulent flow as well as the heat transfer mechanisms in internally finned

http://doi.org/10.30684/etj.2023.140948.1477
Received 12 August 2023; Received in revised form 27 September 2023; Accepted 02 October 2023; Available online 24 October 2023
2412-0758/University of Technology-Iraq, Baghdad, Iraq

tubes, the numerical analysis of Kim et al. [4] created a series of comprehensive flow visualizations. It was found that the tall fin and the micro-fin tubes have various controlling physics. Shome [5] numerically studied the evolution of a mixed convection flow in internally finned tubes with various viscosities. Particularly, it was discovered that the coring makes the tubes with numerous fins or tall fins perform poorly in heat transfer and that the entrance region can significantly improve heat transfer. Viscosity was also found to significantly impact the friction factor and the Nusselt number estimations. Moreover, Dandotiya and Banker [6] designed a Phase Change Material (PCM)-based HE with two new fin configurations, and the improved heat transfer was quantitatively assessed. The fin location was discovered to have a substantial impact on heat transfer.

A feed-forward artificial neural network (ANN) was created by Shabanian et al. [7] to evaluate the thermal performance, the Nusselt number, and the friction factor in a tube with a perforated twisted tape. Furthermore, several better empirical formulae were put out. In order to forecast the temperature and flow properties in a rectangular channel fitted with several twisted tape vortex generators. Beigzadeh et al. [8] used a hybrid model that included a back-propagation network and the genetic algorithm. The created neural networks were discovered to perform better than Ebrahimi and Roohi [9] analysis of the empirical correlations. The mini-twisted oval tubes' internal flow patterns, the statistical heat transmission, and the links between the tube configurations and the overall performance were reported. Promthaisong et al. [10] found that maximum heat rise occurred at certain geometric parameters and operating circumstances. In another study Liu et al. [11] achieved numerical research on the flow characteristics as well as the shell side heat transfer of rod-baffle heat exchangers with spirally corrugated tubes, providing four models for the investigation, including One-start, Two-start, Three-start, and Four-start spirally corrugated tubes in the RBHXsSCT (Rod-baffle HEs with spirally corrugated tubes). The results revealed that compared to RBHX, the heat transfer amounts were larger, and the pressure drops were lower when the Reynolds numbers were between 6,000 and 18,000 for (Rod baffle HEs with plain tubes). When the three-start spirally corrugated tube was used to boost the heat transfer at low Reynolds numbers, it could significantly increase the heat transfer with only a little increase in the friction factor, according to the research by Kareem et al. [12], after experimenting with four-start spirally corrugated tubes concentrated on the non-symmetric nature of the corrugation angles along the longitudinal direction.

Nakhchi et al. [13] investigated heat transfer and pressure drop in double-pipe heat exchangers with perforated elliptical-shaped turbulators. These turbulators improved heat transfer by as much as 9 percent compared to a smooth pipe. Bozkula and Demir [14] investigated the heat transfer and pressure drop characteristics of a finned tube heat exchanger under dry and wet surface conditions, thereby shedding new light on the design and optimization of finned heat exchangers.

Toghraie et al. [15] used a two-phase mixture model to simulate the flow of a ring-shaped water-Al_2O_3 nanofluid in a microscale annulus. They investigated the complex heat transfer in the laminar flow regime. Marzouk et al. [16] examined new helical tube heat exchanger designs via computer simulations and experiments. These designs were up to 42% superior to smooth tubes. Gugulothu and Sanke [17] studied heat transfer in a shell-and-tube heat exchanger with overlapping helical baffles, quantifying the impact of baffle geometry and flow parameters on heat transfer coefficients and pressure drop.

Al-Zahrani [18] conducted experiments to evaluate three new double-pipe heat exchanger designs. Using theoretical models, he compared the heat transfer and friction factors to determine which worked best. Varzaneh et al. [19] examined single-phase and two-phase models to simulate nanofluid flow and heat transfer in a microtube with ribs and a straight cross-section. They discovered that the two-phase model best matched experimental findings. Barnoon et al. [20] used a computer model to examine the heat transfer through a non-Newtonian nanofluid in an inclined, porous cavity with inner cylinders. The heat was transferred using natural convection and thermal radiation. Khodabandeh et al. [21] investigated a new design for a microchannel heat sink with rectangular ribs and sinusoidal cavities. They discovered that water-GNP nanofluids significantly enhanced thermal performance compared to pure water.

This paper aims to study the effect of the corrugated tube and the rod baffle to enhance heat transfer and decrease the shell side's pressure drop. There are numerous applications for this heat exchanger in several engineering fields. Tubes and baffles play an important role in this heat transfer enhancement. By studying the works mentioned above from the literature, it was found that most of these works considered only the smooth tube with some modifications on the baffle type. In addition, most of these works were based on numerical calculations and mathematical models. However, in the present proposed paper, the corrugated tubes and the rod baffle were used to enhance the heat transfer on both sides with an acceptable increase in pressure drop. Heat transfer in tubular heat exchangers is essential in numerous industries, such as power facilities, refrigeration, and automotive applications. Inadequate heat transfer can decrease productivity, increase expenses, and equipment failure [1]. It is crucial to optimize heat exchanger designs for compact equipment footprints. However, predicting heat transfer and pressure drop characteristics in complex geometries such as corrugated tubes can be difficult. Additional experimental research is required to provide design guidance and accurate data for specific applications.

2. Experimental work

2.1 Experimental setup

A shell and tube heat exchanger with interchangeable tube and baffle elements has been developed for testing heat transfer and friction factors. Figure 1 displays the present experimental work. Specifically, the test rig chiefly consists of a water pump, a developing pipe, a water flow pipe, a test section, and an exit section. Moreover, the test section's two types (x/d=1.25 and 1.375) are the shell and the tube HE, which comprises two circular tubes. The inner tube of 16mm in diameter produced from copper was used as a test tube. In addition, the test tube is jacketed via two tubes (20 mm and 22 mm) in diameter. Additionally, the jacket is sealed from the tube's two sides to prevent leakage. The water flow rate throughout the test section was measured by employing two rotometers, one for cold water and the other for hot water. A water U-tube manometer was used to measure pressure drop across the shell side. For evaluating the fluid temperature at the inlet and the exit of the tube side and the shell

side, a thermocouple was connected to a moving jaw of the traverse mechanism for measuring the local temperature and the local dynamic pressure distribution at the exit section. As a result, the temperature of the bulk fluid can be assessed.

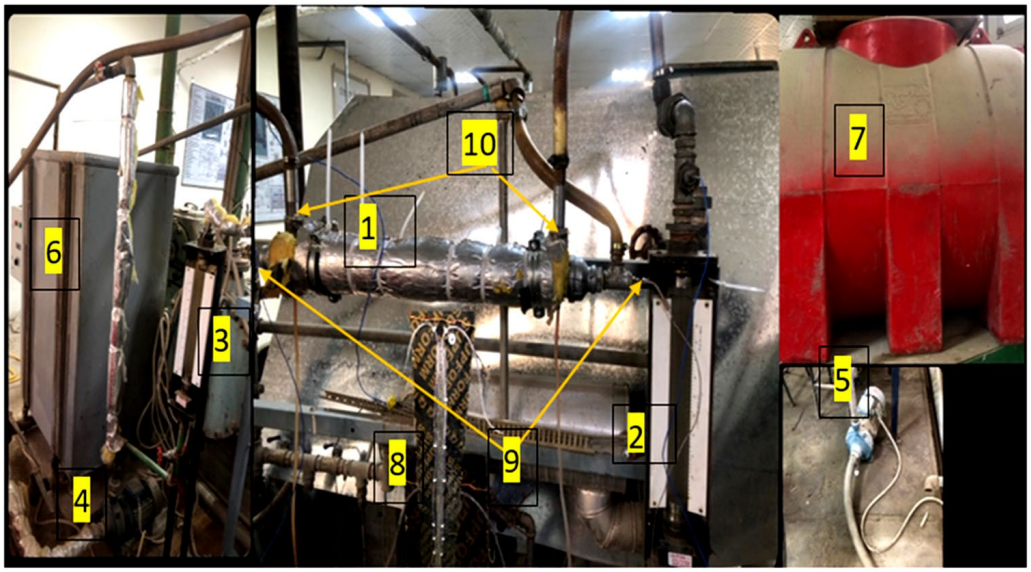

(1) Test section. (2) Flow meter for cold water. (3) Flow meter for hot water. (4) Pump for hot water. (5) Pump for cold water. (6) Water tank for hot water. (7) Water tank for cold water. (9) Thermocouple type (k) for hot pipe. (10) Thermocouple type (k) for cold pipe.

Figure 1: Photo of the test rig

2.2 Tested tubes

The test section is a shell and tube HE, where the cold water flows in the shell side, whereas the hot water flows in the tube side, as shown in Figure 2, and the shell side and the rod baffle with the test section are depicted in Figure 3. Furthermore, the shell side is made from a carbon steel tube having two sizes of 20 mm, and 22 mm inner diameter, 22 mm and 24 mm outer diameter, a length of 1000 mm, and the tube side has a diameter of 16 mm and a length of 1250 mm. The shell ends are welded with a special flange, as illustrated in Table 1.

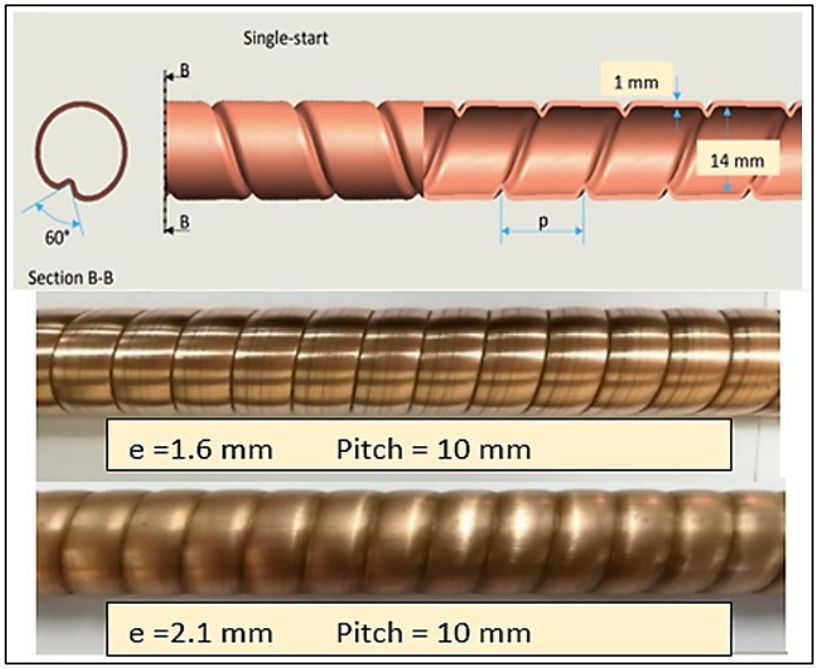

Figure 2: Test section details for the tube side

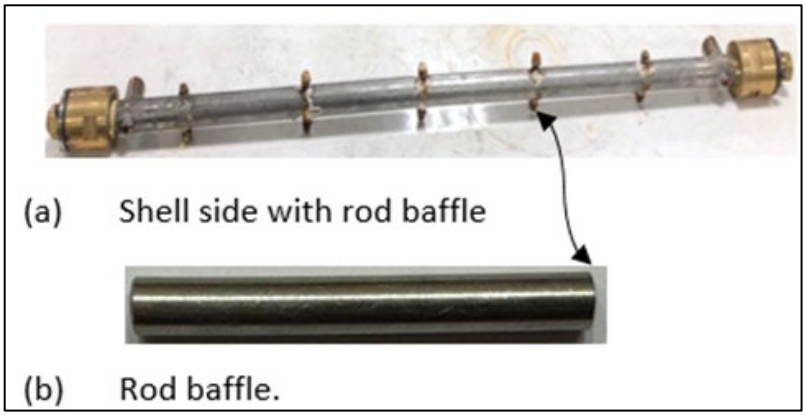

Figure 3: (a) Test section with rod baffle for the sell side (b) rod baffle

Table 1: A group of tested tubes with their dimensions: hydraulic diameter D_h, corrugated depth (e), corrugation pitch (p), dimensionless depth (e/D_h), and dimensionless pitch (p/D_h) for one start

No.	D_h (mm)	e (mm)	P(mm)	e/D_h (-)	P/D_h (-)	Cross-section shape
1	4	-	-	-	-	Smooth tube
2	6	-	-	-	-	Smooth tube
3	4	1.6	10	0.4	2.5	
4	4	2.1	10	0.525	2.5	
5	4	1.6	20	0.4	5	
6	4	2.1	20	0.525	5	
7	4	1.6	30	0.4	7.5	
8	4	2.1	30	0.525	7.5	
9	6	1.6	10	0.266	1.6	
10	6	2.1	10	0.35	1.6	
11	6	1.6	20	0.266	3.33	
12	6	2.1	20	0.35	3.33	
13	6	1.6	30	0.266	5	
14	6	2.1	30	0.35	5	

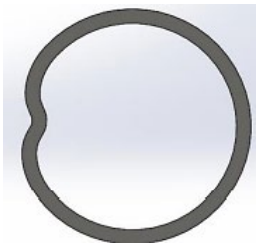

3. Data reduction method

3.1 Nusselt number (*Nu*)

The Equation 1 to calculate the Nusselt number is shown below:

$$Nu = \frac{h_s D_h}{k_{fluid,in\ shell}} \tag{1}$$

3.1.1 Overall heat transfer coefficient (U)

The following expressions are used to compute the overall heat transfer coefficient form Equation 3:

$$\frac{1}{U} = \frac{1}{h_t} + \frac{d_{o,t}}{2*k_t} \ln\frac{d_{o,t}}{d_{i,t}} + \frac{1}{h_{sh}} \frac{d_{o,t}}{d_{i,t}} \tag{2}$$

$$\mathrm{U} = \frac{\mathrm{Q_{ave}}}{\Delta \mathrm{T_m\ F}} \tag{3}$$

3.1.2 Heat transfer average (Q_{ave})

For all testing, the hot and cold-water sides' respective heat transfer rates in Equations 6 and 7 should be less than 5.0 percent. The energy balance equations are as follows in Equations 4 and 5:

$$Q_{hot} = \dot{m}\, c_p\, (T_{h,in} - T_{h,out}) \tag{4}$$

$$Q_{cold} = \dot{m}\, c_p\, (T_{c,out} - T_{c.in}) \tag{5}$$

$$Q_{ave} = \frac{Q_{hot}+Q_{cold}}{2} \quad (6)$$

$$\left|\frac{Q_{hot}- Q_{cold}}{Q_{ave}}\right| \leq 5\% \quad (7)$$

3.1.3 Logarithmic mean temperature difference (ΔT_m)

The logarithmic mean temperature difference in Equation 8, which is more accurate than the average temperature difference, is calculated as follows:

$$\Delta T_m = \frac{(T_{hot,in}-T_{cold,out})-(T_{hot,out}-T_{cold,in})}{\ln(T_{hot,in}-T_{cold,out})/(T_{hot,out}-T_{cold,in})} \quad (8)$$

3.1.4 The heat transfer area of the tested heat exchanger is calculated as:

The heat transfer area outside the tubes is calculated in Equation 9 as follows:

$$F = \pi\, d_{out,t}\, L \quad (9)$$

while the heat exchanger's fouling resistance is disregarded, the overall heat transfer coefficient of the heat exchanger based on the outer surface area is as expressed below:

$$h_t = 0.023 \frac{k_t}{d_{o,t}} Re^{0.8} Pr^{0.33} \quad (10)$$

$$h_t = 0.044 \frac{k_t}{d_h}\left(\frac{e}{d_h}\right)^{0.2374}\left(\frac{p}{d_h}\right)^{0.01106}\left(\frac{90^\circ-\theta}{90^\circ}\right)^{0.5786} Re^{0.8575} Pr^{0.33} \quad (11)$$

The Dittus-Boelter correlation for the smooth tube is used to obtain the tube-side heat transfer coefficient, as illustrated in Equation 10 [13], while for the corrugated tubes, Equation 11 is used [14].

3.1.5 Hydraulic diameter is calculated as:

The hydraulic diameters mentioned above are all calculated using the following Equation 12:

$$D_h = \frac{A_c}{P(wetted)} \quad (12)$$

The reference temperature for the computation of the physical parameters is the bulk temperature value of the inlet and outlet temperatures in the test section in Equation 13:

$$T_b = \frac{T_{in}+T_{out}}{2} \quad (13)$$

3.2 Calculation of the friction factor

Due to the low-temperature increase across the test section (T_{out} -T_{in} < 50°C), the shear force along the tube is constant. It is a function of velocity and viscosity variation due to temperature gradient since the process is adiabatic. On the other hand, the water static pressure drop would convert into friction losses and increase kinetic energy. Therefore, the friction factor (*f*) can be calculated directly from the Darcy equation [22] in Equation 14:

$$f = \frac{D_h}{l}\frac{2\,\Delta P}{\rho_w V^2} \quad (14)$$

Mean velocity is computed in Equation 15 as:

$$V = \frac{\dot{m}}{\rho_w A_c} \quad (15)$$

Reynolds number is calculated based on the hydraulic diameter in Equation 16 as:

$$Re = \frac{\rho_w V {D_h}^2}{\mu} \quad (16)$$

4. Results and discussion

4.1 Verification of the smooth tube

The reliability of data acquired from the experimental setup was validated by performing tests on the smooth tube and then evaluating the heat transfer and pressure losses in terms of the Nusselt number and the isothermal friction factor. Then, the isothermal friction factor and the Nusselt number data were compared with widespread standard correlations available in the literature. The standard results of the Nusselt number and the friction factor for the turbulent flow through the smooth tube were estimated from the following correlations proposed by Ginilski [23] for the Nusselt number and Filonenko [24] for the friction factor, see Figures 4 and 5 for Nusslet number , Figures 6 and 7 for the friction factor for (X/D=1.25) and (X/D=1.375) respectively:

$$Nu = \frac{\left(\frac{f}{8}\right)(Re-1000)Pr}{1+12.7\left(\frac{f}{8}\right)^{0.5}\left(Pr^{\frac{2}{3}}-1\right)}\left[1+\left(\frac{d}{L}\right)^{\frac{2}{3}}\right]\left(\frac{Pr}{Pr_w}\right)^{0.11} \quad (17)$$

$$f = (1.28\log_{10} Re - 1.64)^{-2} \quad (18)$$

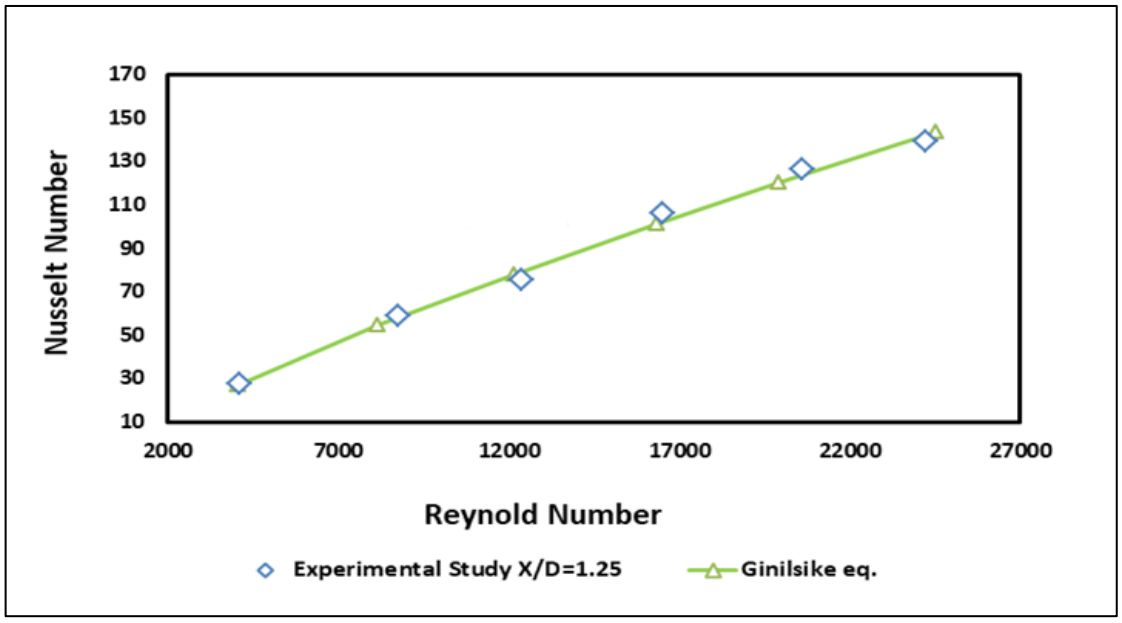

Figure 4: Relationship between experimental study and Ginilsike equation with error (-2, +3) for (X/D=1.25)

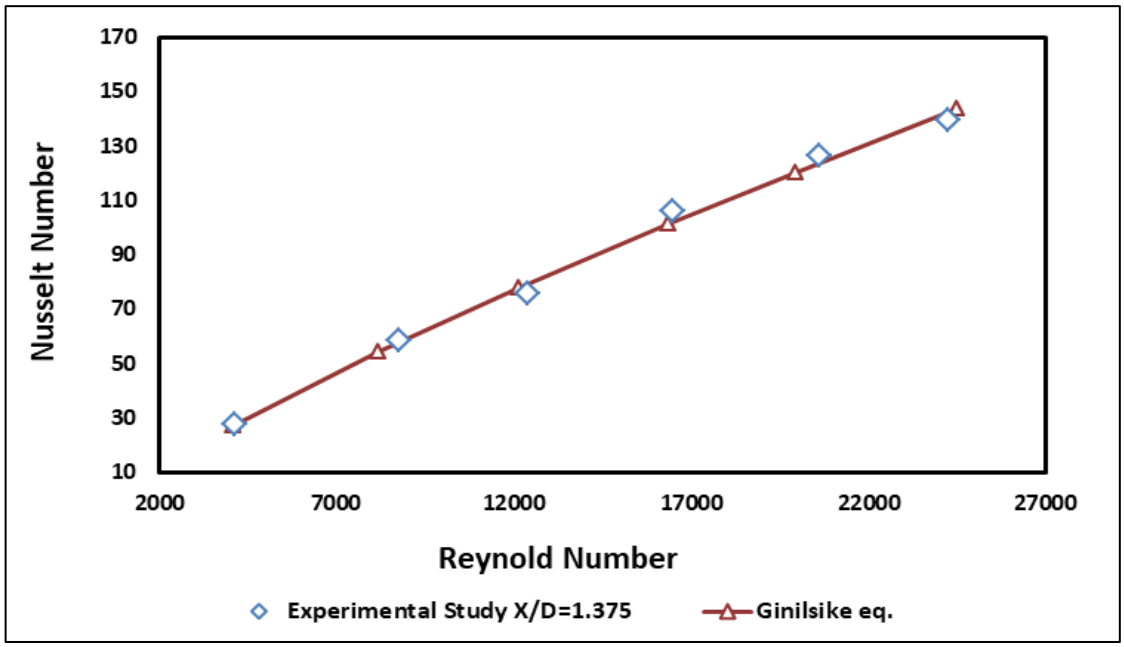

Figure 5: Relationship between experimental study and Ginilsike equation with error (-3, +4) for (X/D=1.375)

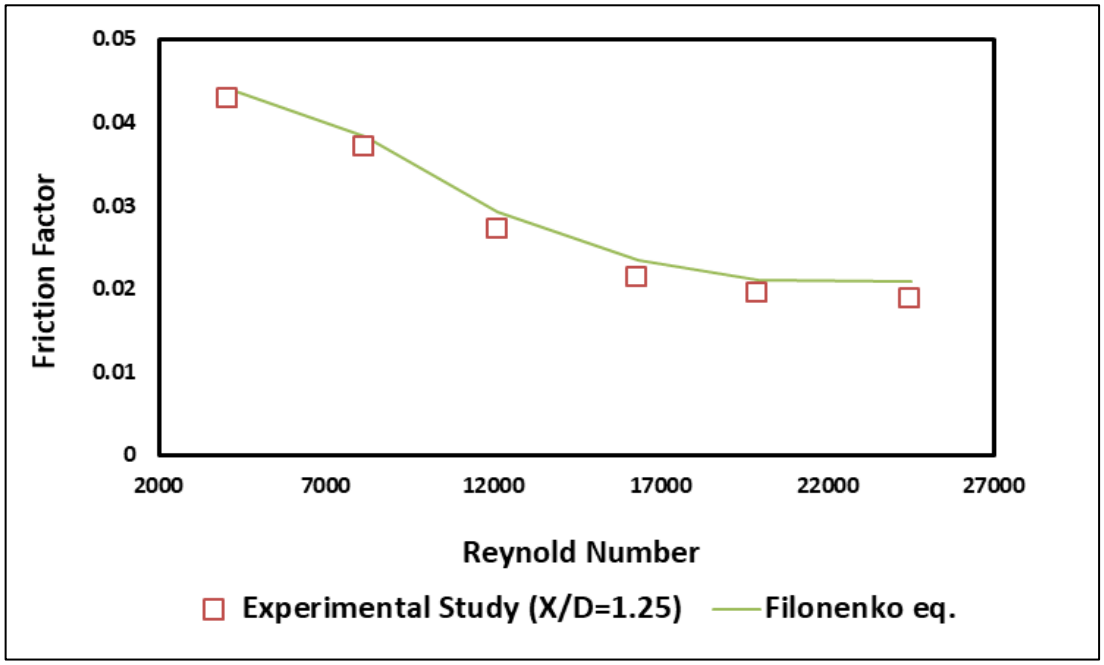

Figure 6: Relationship between experimental study and Filonenko equation with error (-3, +2) for (X/D=1.25)

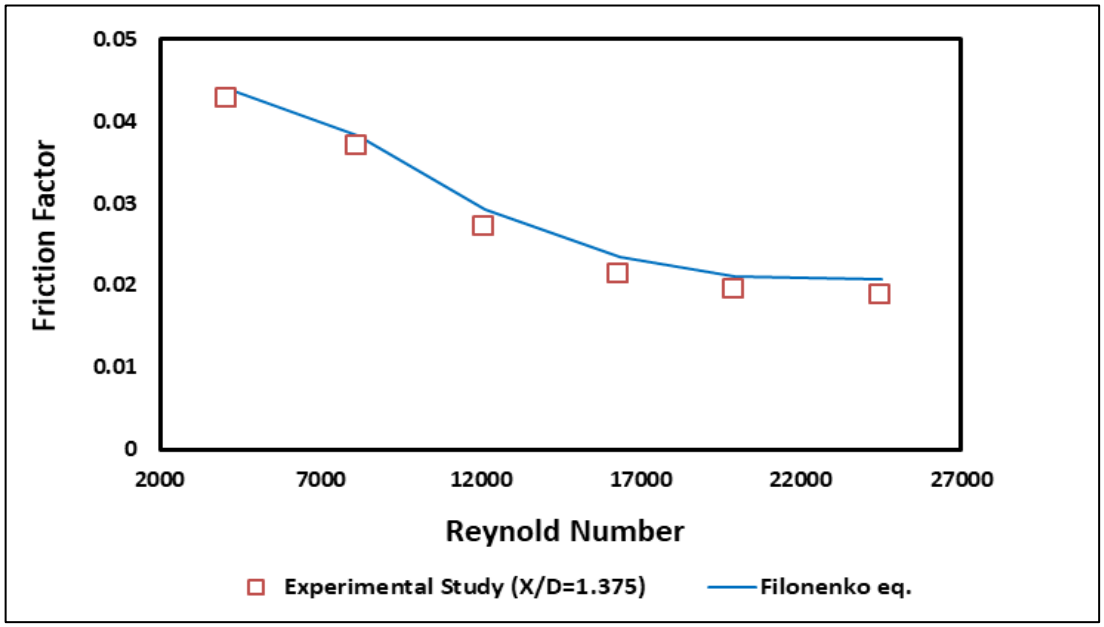

Figure 7: Relationship between experimental study and Filonenko equation with error (-3, +2) for (X/D=1.375)

4.2 Heat transfer

Corrugated tubes with a smaller pitch and higher depth enhance heat transfer but increase pressure drop. Rod baffles improve heat transfer but add pressure drop. Tube corrugations can cause flow disturbances, thermal boundary layer cracking, and rod baffles. As a result, they widen the temperature gap between the surface temperature and the nearby flow temperature. Figure 8 for (X/D =1.25) and Figure 9 for (X/D =1.375) depict the impact of a groove for (1-star) tubes without a rod baffle on the rate of heat transfer in terms of the Nusselt number at the maximum depth of the groove (dg=2.1 mm). The results demonstrated that the depth significantly affects the heat transfer because the greater thickness of the boundary layer of a smooth tube is created at low Reynolds numbers.

Flow disruption and thermal boundary layer rupture are typical in tubes with corrugations. In order to do this, the temperature gap between the surface temperature and the nearby flow temperature has to be widened. The Figures mentioned above reveal the influence of a groove for one-star tubes with a rod baffle at the maximum depth of the groove (e= 2.1 mm) on the rate of heat transfer in terms of the Nusselt number. The findings indicated that the depth significantly affects the heat transfer because the smooth tubes with low Reynolds numbers cause the boundary layers to be thicker. In the corrugated tube, the smaller corrugation pitch (p) in the same (e/d) provide a higher Nusselt number than that of the smooth tube over the whole range of Reynolds number. This effect is due to the high flow mixing induced at this smaller pitch, as illustrated in Figures 10 and 11.

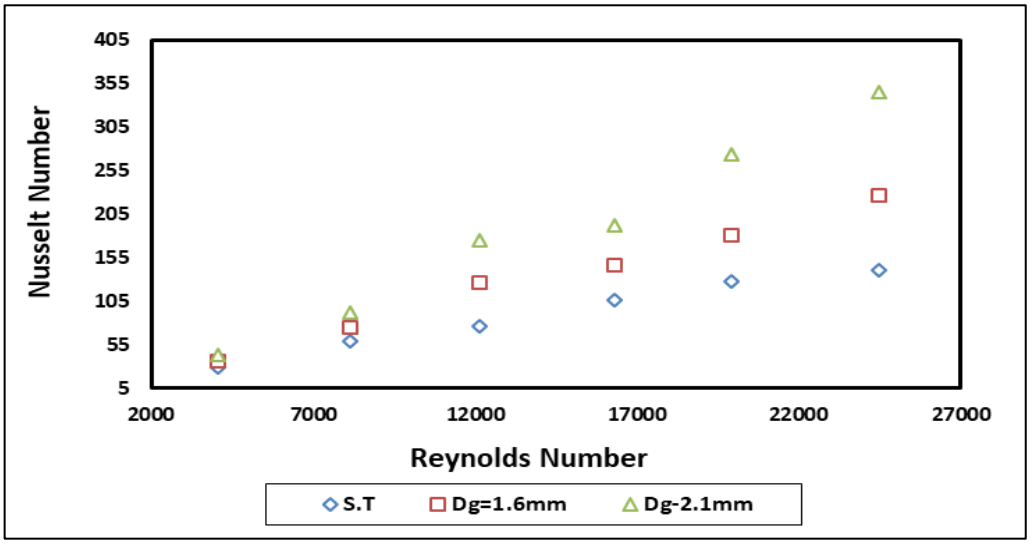

Figure 8: The Reynolds number versus the Nusselt number for the smooth pipe and different depth grooved pipes with (x/d=1.25) at pitch=10 mm

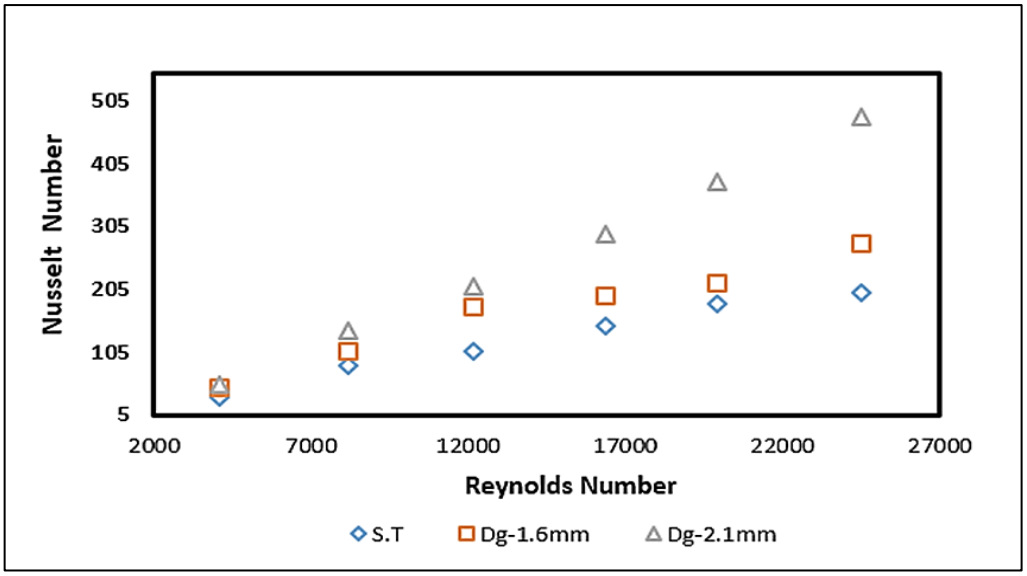

Figure 9: The Reynolds number versus the Nusselt number for the smooth pipe and different depth grooved pipes with (x/d=1.375) at pitch=10 mm

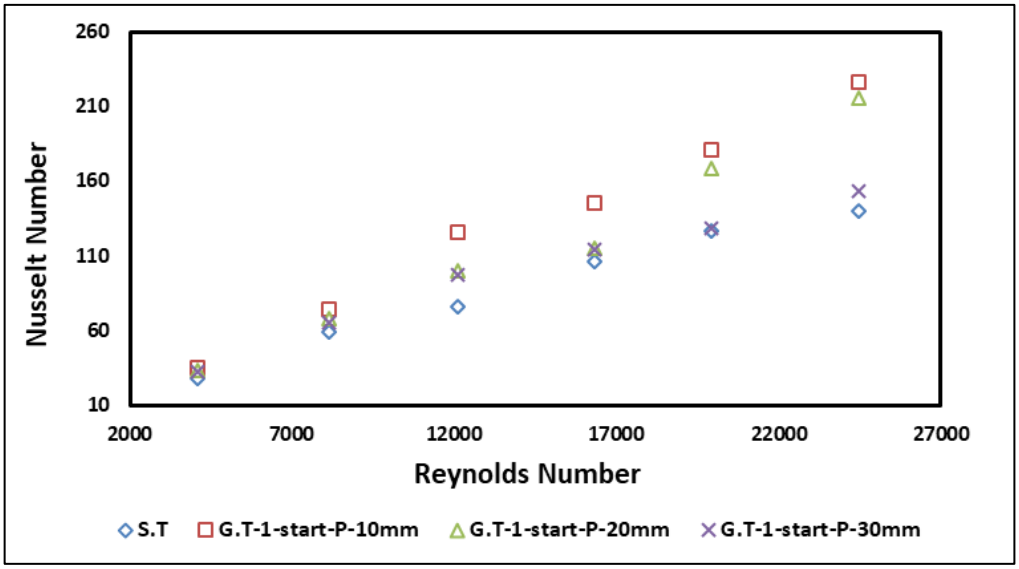

Figure 10: The Reynolds number versus the Nusselt number for the smooth pipe and the grooved pipes with (x/d=1.25) and pitch=10, 20 and 30 mm

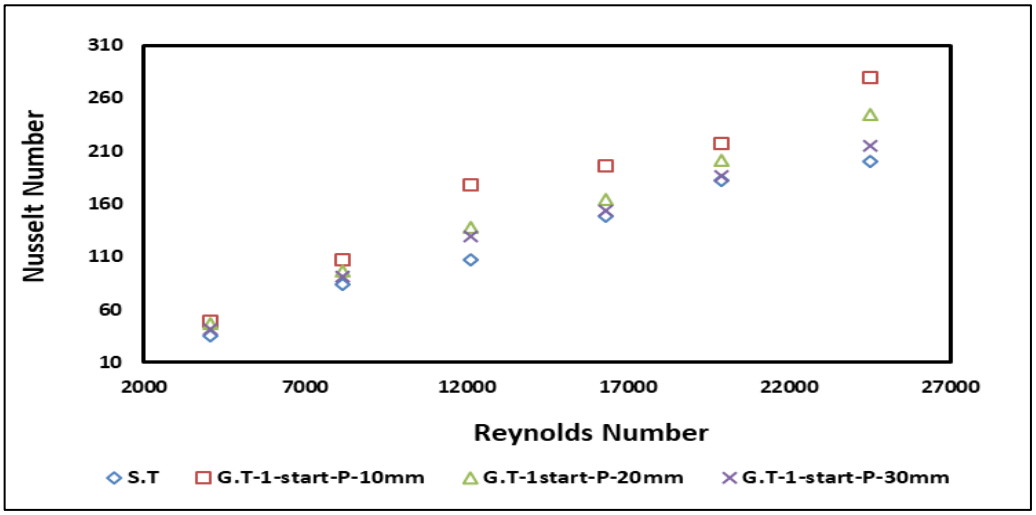

Figure 11: The Reynolds number versus the Nusselt number for the smooth and grooved pipes with (x/d=1.375) and pitch=10, 20 and 30 mm

4.3 Friction factor

The flow in the shell side is very challenging. Nevertheless, the outer surface of the corrugated tubes and the rod baffle cause flow obstruction. The pressure drop across the corrugated tube resulted because of the following Figures in 12 (a- d):

1) The drag forces applied to the flow of fluid via the helical rib.
2) The rotational flow produced via the helical rib.
3) The frictional drag augmentation.
4) The flow obstruction caused by a decrease in the tube's cross-sectional area.

However, the pressure drop caused by drag in this tube type is the main issue since the corrugated surface obstructs the flow direction. Each of these variables would simultaneously affect the pressure drop values and the friction factor. Still, the rod baffle significantly increases the pressure drop, as shown in Figures 12 (a- d).

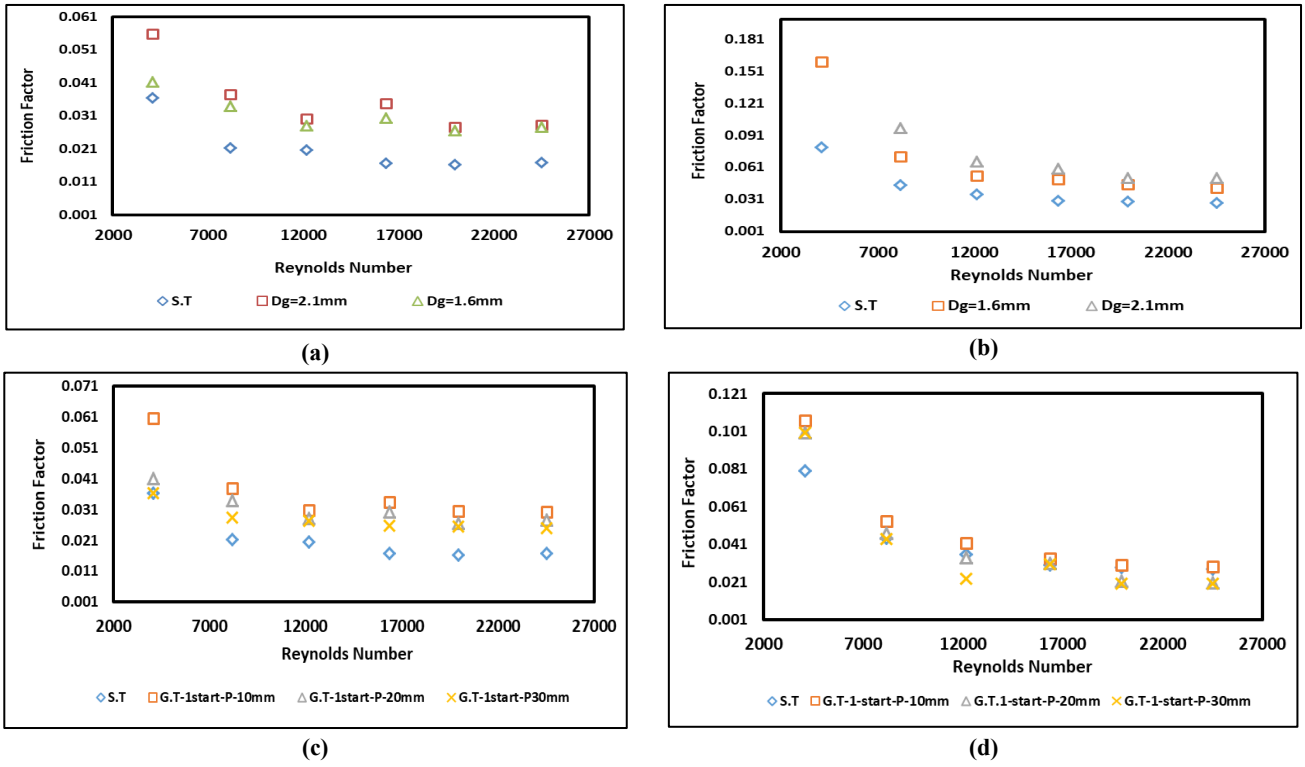

Figure 12: (a) The Reynolds number versus the friction factor for the smooth pipe and different depth grooved pipes with (x/d=1.25) and pitch=10 mm, (b) The Reynolds number versus the friction factor for the smooth pipe and different depth grooved pipes with (x/d=1.375) and pitch=10 mm, (c) The Reynolds number versus the friction factor for the smooth and grooved pipes with (x/d=1.25) and pitch=10, 20 and 30 mm, (d) The Reynolds number versus the friction factor for the smooth and grooved pipes with (x/d=1.375) and pitch=10, 20, and 30 mm

4.4 Thermal enhancement factor

This factor is one of the most comprehensive comparative factors. The best purpose of PEC is probably to select the optimized design and operating conditions for different heat exchanger types. For evaluating the rough surface performance, [25] proposed the criterion of T.E.F., which describes the heat transfer increase of the improved tube compared to that of the smooth tube at the fixed pumping power in terms of the Nusselt number.

Figures 13 and 14 display the thermal enhancement factor for the grooved pipes with pitch=10, 20, and 30mm for (x/d=1.25 and 1.375), respectively.

$$T.E.F = \frac{\frac{Nu}{Nu_s}}{(\frac{f}{f_s})^{1/3}} \quad (17)$$

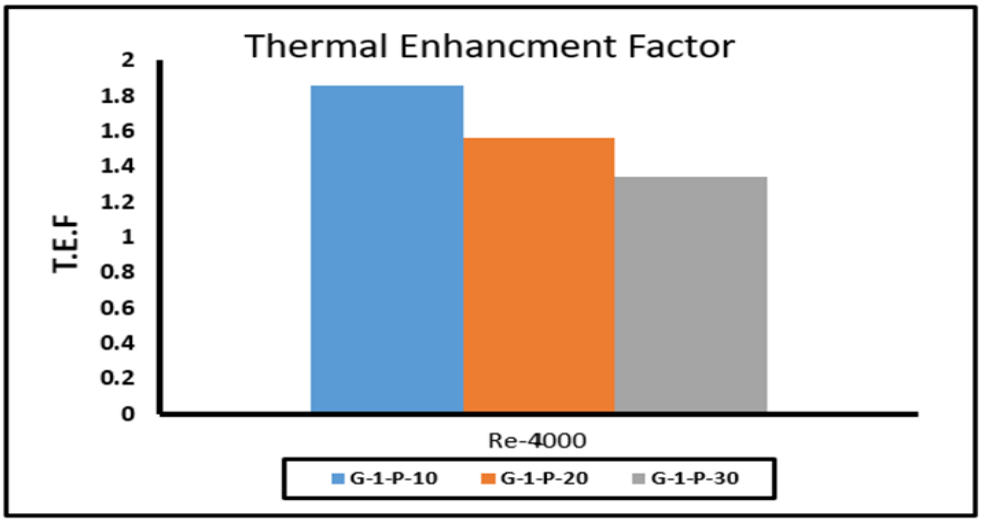

Figure 13: Thermal enhancement factor for the grooved pipes with pitch=10, 20, and 30mm for (x/d=1.25) at Reynolds Number of (4000)

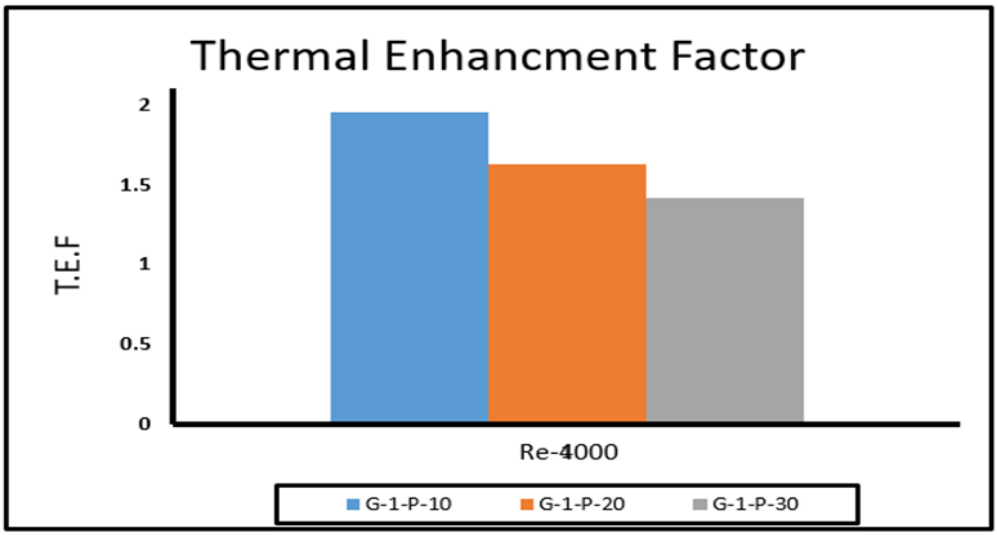

Figure 14: Thermal enhancement factor for the grooved pipes with pitch=10, 20, and 30mm for (x/d=1.375) at Reynolds Number of (4000)

5. Conclusion

The research investigated corrugated tubes with rod baffles and water as the working fluid on the shell side of a heat exchanger. The Reynolds number range was evaluated in the turbulent region between 4,000 and 24,000 Reynolds. The study utilized water as its working fluid and varied corrugation depths. Key findings include:

- Compared to smooth tubes, corrugated tubes enhanced heat transfer, improving depth. At maximum depth, the average Nusselt number rose by 55% and 59% at the smallest pitch due to flow-disrupting corrugations and thermal boundary layer breakdown caused by the smallest pitch.
- According to the study, decreasing the corrugation pitch (p) from 30 mm to 10 mm increased the Nusselt number by 25% for x/d = 1.25 and 38% for x/d = 1.375, resulting in greater heat transfer.

- It was discovered that the friction factor of corrugated tubes is significantly greater than that of smooth tubes, increasing by 66–130% depending on depth and reducing with pitch and x/d ratio.
- With a fixed pumping power, the optimal configuration for optimizing heat transfer without excessive pressure drop was achieved, yielding a maximum thermal enhancement factor of 1.97.
- Rod baffles improve heat transfer and pressure drop, complementing corrugated tubes for improved heat transfer on the shell side.

In summary, the research indicates that corrugated tubes with a small pitch and a large depth, combined with rod baffles, can significantly improve the performance of tubular heat exchangers. It recommends choosing optimal geometries to maximize heat transfer and manage pressure drop tradeoffs.

Nomenclature:

Ac	Cross-sectional area
Cp	specific heat
d	Tube diameter
Dh	Hydraulic diameter
e	Corrugation depth
F	heat transfer area outside the tubes (annuals)
f	Darcy-Weisbach friction factor
G	Fluid mass velocity
h	Average heat transfer coefficient
v	Fluid specific volume
k	Thermal conductivity
L	Length
P	Corrugation pitch
Q	Rate of heat transfer
$\dot{m}$	Mass flow rate
P	Wetted
T	the temperature
v	Flow velocity component

Greek symbols

θ	Corrugation angle
μ	Dynamic viscosity of fluid
ρ	Fluid density
Δp	Pressure drop
ΔT	Logarithmic mean temperature difference

Subscript

C	cold water
b	the bulk temperature
h	hot water
i	Horizontal direction in Inlet fluid
m	mean
o	Outer side out
s	Smooth tube
t	tube
w	water

Dimensionless numbers

Pr	Prandtal number
Nu	Nusselt number
Re	Reynolds number

Author contributions

Conceptualization, N. Fadhil, A. Al-dabagh and F. Hatem; methodology, A. Al-dabagh; software, N.Fadhil and A. Al-dabagh; validation, N.Fadhil, A. Al-dabagh and F. Hatem; formal analysis, N. Fadhil; investigation, N. Fadhil; resources, N. Fadhil; data curation, N. Fadhil and A. Al-dabagh; writing—original draft preparation, N. Fadhil and A. Al-dabagh; writing—review and editing, N.Fadhil, A. Al-dabagh and F. Hatem; visualization, N.Fadhil; supervision, A. Al-dabagh. and F. Hatem; project administration, A. Al-dabagh. All authors have read and agreed to the published version of the manuscript.

Funding

This research received no specific grant from any funding agency in the public, commercial, or not-for-profit sectors.

Data availability statement

The data that support the findings of this study are available on request from the corresponding author.

Conflicts of interest

The authors declare that there is no conflict of interest.

References

[1] M. A. Pakhomov and V. I. Terekhov, Numerical modeling of turbulent flow structure and heat transfer in a droplet-laden swirling flow in a pipe with a sudden expansion, Numer. Heat Transf. A: Appl., 71 (2017) 721–736. https://doi.org/10.1080/10407782.2017.1308740

[2] I. Petracci, M. Luca, and G. Fabio, Numerical simulation of the optimal spacing for a radial finned tube cooled by a rectangular jet. I – average thermal results, Int. J. Therm. Sci., 104 (2016) 54–67. https://doi.org/10.1016/j.ijthermalsci.2016.01.001

[3] G. Ravi, L. J. Alvarado, C. Marsh, and D. A. Kessler, Laminar flow forced convection heat transfer behavior of a phase change material fluid in finned tubes, Numer. Heat Transf. A: Appl., 55 (2009) 721–738. https://doi.org/10.1080/10407780902864672

[4] J. H. Kim, K. E. Jansen, and M. K. Jensen, Analysis of heat transfer characteristics in internally finned tubes, Numer. Heat Transfer A. 46 (2004) 1–21. http://dx.doi.org/10.1080/10407780490454296

[5] B. Shome, Mixed convection laminar flow and heat transfer of liquids in horizontal internally finned tubes, Numer. Heat Transfer A. 33 (1998) 65–83. https://doi.org/10.1080/10407789808913928

[6] D. Dandotiya and N. D. Banker, Numerical investigation of heat transfer enhancement in a multitube thermal energy storage heat exchanger using fins, Numer. Heat Transfer A. 72 (2017) 389–400. https://doi.org/10.1080/10407782.2017.1376976

[7] S. R. Shabanian, I. Shiva, and T. Hatami, Application of intelligent methods for the prediction and optimization of thermal characteristics in a tube equipped with perforated twisted tape, Numer. Heat Transfer A. 70 (2016) 30–47. http://dx.doi.org/10.1080/10407782.2016.1139982

[8] R. Beigzadeh, M. Rahimi, M. Parvizi, and S. Eiamsa, Application of ann and Ga for the prediction and optimization of thermal and flow characteristics in a rectangular channel fitted with twisted tape vortex generators, Numer. Heat Transfer A. 65 (2014) 186–199. https://doi.org/10.1080/10407782.2013.826010

[9] A. Ebrahimi and E. Roohi, Numerical study of flow patterns and heat transfer in mini twisted oval tubes, Int. J. Mod. Phys. C. 26 (2015) 1–18. https://doi.org/10.1142/S0129183115501405

[10] P. Promthaisong, W. Jedsadaratanachai, and S. Eiamsa-ard, 3D numerical study on the flow topology and heat transfer characteristics of turbulent forced convection in a spirally corrugated tube, Numer. Heat Transfer A., 69 (2016) 607–629. https://doi.org/10.1080/10407782.2015.1069670

[11] J. Lu, X. Sheng, J. Ding, and J. Yang, Transition and turbulent convective heat transfer of molten salt in spirally grooved tube, Exp. Therm. Fluid Sci., 47 (2013) 180–185. https://doi.org/10.1016/j.expthermflusci.2013.01.014

[12] Z. S. Kareem, S. Abdullah, and T. M. Lazim, Heat transfer enhancement in three-start spirally corrugated tube: experimental and numerical study, Chem. Eng. Sci., 134 (2015) 746–757. https://doi.org/10.1016/j.ces.2015.06.009

[13] M. E. Nakhchi, M. Hatami, and M. Rahmati, Experimental investigation of performance improvement of double-pipe heat exchangers with novel perforated elliptic turbulators, Int. J. Therm. Sci., 168 (2021) 107057. https://doi.org/10.1016/j.ijthermalsci.2021.107057

[14] G. Bozkula and H. Demir, Experimental investigation of heat transfer and pressure drop of fin and tube heat exchanger under dry and wet conditions, Int. J. Therm. Sci., 177 (2022) 107580. https://doi.org/10.1016/j.ijthermalsci.2022.107580

[15] D. Toghraie, R. Mashayekhi, H. Arasteh, S. Sheykhi, M. Niknejadi, and A. J. Chamkha, Two-phase investigation of water-Al2O3 nanofluid in a micro concentric annulus under non-uniform heat flux boundary conditions, Int. J. Numer Methods Heat Fluid Flow, 30 (2019) 1795–1814. https://doi.org/10.1108/HFF-11-2018-0628

[16] S. A. Marzouk, M. M. Abou Al-Sood, E. M. S. El-Said, M. K. El-Fakharany, and M. M. Younes, Study of heat transfer and pressure drop for novel configurations of helical tube heat exchanger: a numerical and experimental approach, J. Therm. Anal. Calorim., 148 (2023) 1–16. https://doi.org/10.1007/s10973-023-12067-7

[17] R. Gugulothu and N. Sanke, Experimental investigation of heat transfer characteristics for a shell and tube heat exchanger, Energy Harvesting Syst., 2023. https://doi.org/10.1515/ehs-2022-0147

[18] S. Al-Zahrani, Heat transfer characteristics of innovative configurations of double pipe heat exchanger, Heat Mass Transfer, 59 (2023) 1661-1675. https://doi.org/10.1007/s00231-023-03360-0

[19] A. A. Varzaneh, D. Toghraie, and A. Karimipour, Comprehensive simulation of nanofluid flow and heat transfer in straight ribbed microtube using single-phase and two-phase models for choosing the best conditions, J. Therm. Anal. Calorim., 139 (2020) 701–720. https://doi.org/10.1007/s10973-019-08381-8

[20] P. Barnoon, D. Toghraie, R. B. Dehkordi, and M. Afrand, Two phase natural convection and thermal radiation of Non-Newtonian nanofluid in a porous cavity considering inclined cavity and size of inside cylinders, Int. Commun. Heat Mass Transfer., 108 (2019) 104285. https://doi.org/10.1016/j.icheatmasstransfer.2019.104285

[21] E. Khodabandeh, S. A. Rozati, M. Joshaghani, O. A. Akbari, S. Akbari, and D. Toghraie, Thermal performance improvement in water nanofluid/GNP–SDBS in novel design of double-layer microchannel heat sink with sinusoidal cavities and rectangular ribs, J. Therm. Anal. Calorim., 136 (2019) 1333–1345. https://doi.org/10.1007/s10973-018-7826-2

[22] Y. A. Cengel, Heat tranfer a practical approach: McGraw-Hill, 2003.

[23] A. M. Al-dabagh, Falah F. Hatem, Ibrahim E. Sadiq, Effect of Corrugation Depth on Heat Transfer Enhancement and Flow Characteristics for Corrugated Tubes, J. Univ. Babylon Eng. Sci., 26 (2018) 164-181.

[24] G. K. Filonenko, Hydraulic resistance in pipes, Teploenergetika 4 (1954) 40– 44.

[25] A. Bergles, A. Blumenkrantz, and J.Taborek, Performance evaluation criteria for enhanced heat transfer surfaces, Heat transfer, 2 (1974) 239-243.